Photo-Orientation Phenomena in Photochromic Liquid Crystalline Azobenzene-Containing Polymethacrylates with Different Spacer Length

Alexey Bobrovsky,* Valery Shibaev, Alexey Piryazev, Denis V. Anokhin, Dimitri A. Ivanov, Olga Sinitsyna, Vera Hamplova, Miroslav Kaspar, Alexej Bubnov

Synthesis and investigation of the phase behavior and photo-optical properties of two chiral liquid-crystalline polymers with azobenzene-containing side groups having different spacer lengths, 6 and 10 methylene groups (**PMAzo-6** and **PMAzo-10**, respectively) are described. Formation of different smectic phases and high-temperature cholesteric phase is studied by polarizing optical microscope, differential scanning calorimetry, and X-ray investigations. It is shown that UV-irradiation induces effective reversible *E–Z* photoisomerization in polymer solutions and films. Atomic force microscopy (AFM) study reveals substantial changes in the surface topography of the polymer **PMAzo-6** film after UV-irradiation, whereas **PMAzo-10** surface remains the same. Irradiation by polarized light (457 nm) results in photo-orientation process in polymer films consequential in significant alignment of the chromophores in direction perpendicular to the polarization plane of the incident light. A significant difference is found in thermal stability of the photoinduced alignment; an annealing of **PMAzo-10** irradiated samples results in a slight decrease of dichroism values (down to 0.57); whereas the dichroism increases up to very high values (0.91) for **PMAzo-6**.

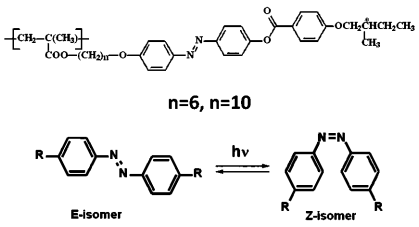

1. Introduction

Photochromic liquid-crystalline (LC) polymers represent a promising type of smart materials with high potential for a large variety of applications in optics and optoelectronics.[1,2] Among different types of photochromic fragments incorporated in polymer matrices, the azobenzene moieties are the most remarkable chromophores

Prof. A. Bobrovsky, Prof. V. Shibaev, Dr. O. Sinitsyna
Faculty of Chemistry
Moscow State University
Leninskie gory, Moscow 119991, Russia
E-mail: bbrvsky@yahoo.com
A. Piryazev, Dr. D. V. Anokhin, Prof. D. A. Ivanov
Faculty of Fundamental Physical and Chemical Engineering
Moscow State University
Leninskie gory, Moscow 119991, Russia
Dr. D. V. Anokhin
Institute of Problems of Chemical Physics RAS
Semenov Prospect 1
Chernogolovka, Moscow region 142432, Russia
Prof. D. A. Ivanov
Institut de Sciences des Matériaux de Mulhouse
CNRS UMR 7361, Jean Starcky 15, F-68057 Mulhouse France
Dr. V. Hamplova, Dr. M. Kaspar, Dr. A. Bubnov
Institute of Physics
The Czech Academy of Sciences
182 21 Prague 8, Czech Republic

Macromol. Chem. Phys. **2017**, DOI: 10.1002/macp.201700127

capable of reversible *E–Z* isomerizing. Several unique advantages of the azobenzene molecules make them the most popular photochrome, such as high quantum yield of photoisomerization, high fatigue resistance, and extreme change in the shape as well as in dipole moment during isomerization.[1–4] Photoisomerization of azobenzene fragments in LC media enables to realize isothermal phase transitions.[5–12] From the other hand, an action of polarized light induces photo-orientation processes and alignment of chromophores in direction perpendicular to the polarization plane of the incident light.[13–20]

Another interesting direction of the research is connected with investigation of the surface topography of LC polymer systems and, especially, manipulation of surface relief by light irradiation. In a number of previous works, the ability of light control of surface topography has been demonstrated.[21–24] In the other words, photoinduced changes in the polymer film structure can result not only in a change of their optical properties, but also in transformation of the surface relief. This effect opens the way for practical applications of such photochromic polymers for creation of smart surfaces.

Despite significant progress in the research of azobenzene-containing LC-systems,[25–28] great potential for applications in photonics, data storage,[29,30] photoactuation,[31–33] there are still many open issues regarding the influence of the chemical structure of LC polymers and their mesophase behavior on photoisomerization and photo-orientation processes.

In the present work, we synthesized and studied two new chiral side-chain azobenzene-containing polymethacrylates having different lengths of the spacer, 6 and 10 methylene units (denoted as **PMAzo-6** and **PMAzo-10**, respectively), Scheme 1.

The main objective of this work is to perform the comparative study of the mesophase structure and photo-optical properties of two polymers in order to elucidate the effect of the spacer length (i) on the mesomorphic behavior and (ii) on kinetics of the photoinduced processes in polymer films. Special attention is paid to exploration of the possibility of manipulation of the degree of LC-order by UV-irradiation and to control the processes of the photo-orientation induced by the action of polarized light. Results concerning the effect of light irradiation on the surface topography of the LC polymer films will be also presented and discussed.

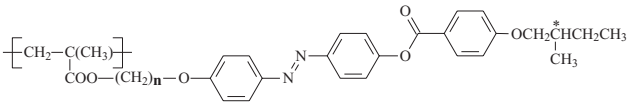

n=6, **PMAzo-6**
n=10, **PMAzo-10**

Scheme 1. Structure of the azobenzene-containing polymethacrylates.

2. Experimental Section

2.1. Synthesis of MAzo-6 and MAzo-10 Monomers

Design of **MAzo-6** monomer as starting material for resulting polymethacrylate was done according to general synthetic procedure represented in Figure 1. Detailed description of the specific reactions and steps together with ^{1}H-NMR spectra of the intermediates and final products are presented in the Supporting Information. Monomer **MAzo-10** was prepared by similar way and its molecular structure was confirmed by measurements of ^{1}H-NMR spectra acquired on a spectrometer Varian 300 MHz in deuterochloroform as well.

The chemical purity of both materials was checked by high pressure liquid chromatography, which was carried out using a silica gel column (Bioshere Si 100-5 μm, 4 × 250, Watrex) with a mixture of 99.9% of toluene and 0.1% of methanol as an eluent, and detection of the eluting products by a UV–vis detector (λ = 290 nm). The chemical purity was found between 99.5% and 99.7%.

2.2. Polymerization

Photochromic polymers were prepared by a radical polymerization of corresponding methacrylic monomers (see the previous section) in benzene solution in the presence of 2 wt% (to monomer) of azobisisobutyronitrile (AIBN). After 3 d storage at 65 °C, the solvent was evaporated and solid product was washed several times by boiling ethanol. Yield of polymerization was about 70%. Such relatively low yield is explained by competing radical transfer reaction promoted by azobenzene fragment. During polymer synthesis, a lot of low-molar-mass products (dimers, short oligomers) are formed. Molecular masses (M_w) and polydispersity of polymers (M_w/M_n) were determined by gel permeation (GPC) chromatography using "Knauer" instrument.

2.3. Mesomorphic Behavior, Structural Properties, and Selective Light Reflection

The phase transition temperatures of the monomers and polymers were measured by differential scanning calorimetry (DSC) using a Perkin Elmer DSC 8500. Dry nitrogen was purged through the DSC cell in order to stabilize the temperature. Standard aluminum pans with about 10 mg of sample material were used. The measurement program started from heating the sample from room temperature to 260 °C at a 10 °C min^{-1} rate, followed by isothermal segment for 1 min, cooling to room temperature, another isothermal segment, and a second heating ramp.

Polarizing optical microscope (POM) investigations in order to determine the type of existing mesophases were performed using LOMO P-112 and Carl Zeiss Discovery V8 polarizing microscopes equipped by Mettler TA-400 heating stage. UV cut-off filter was used for preventing *E–Z* isomerization of azobenzene chromophores during POM observations.

In order to determine the mesophase structure, the X-ray diffraction studies were performed on monomers using Bruker Nanostar system (CuKα radiation, Vantec 2000 area detector,

Macromol. Chem. Phys. **2017**, DOI: 10.1002/macp.201700127

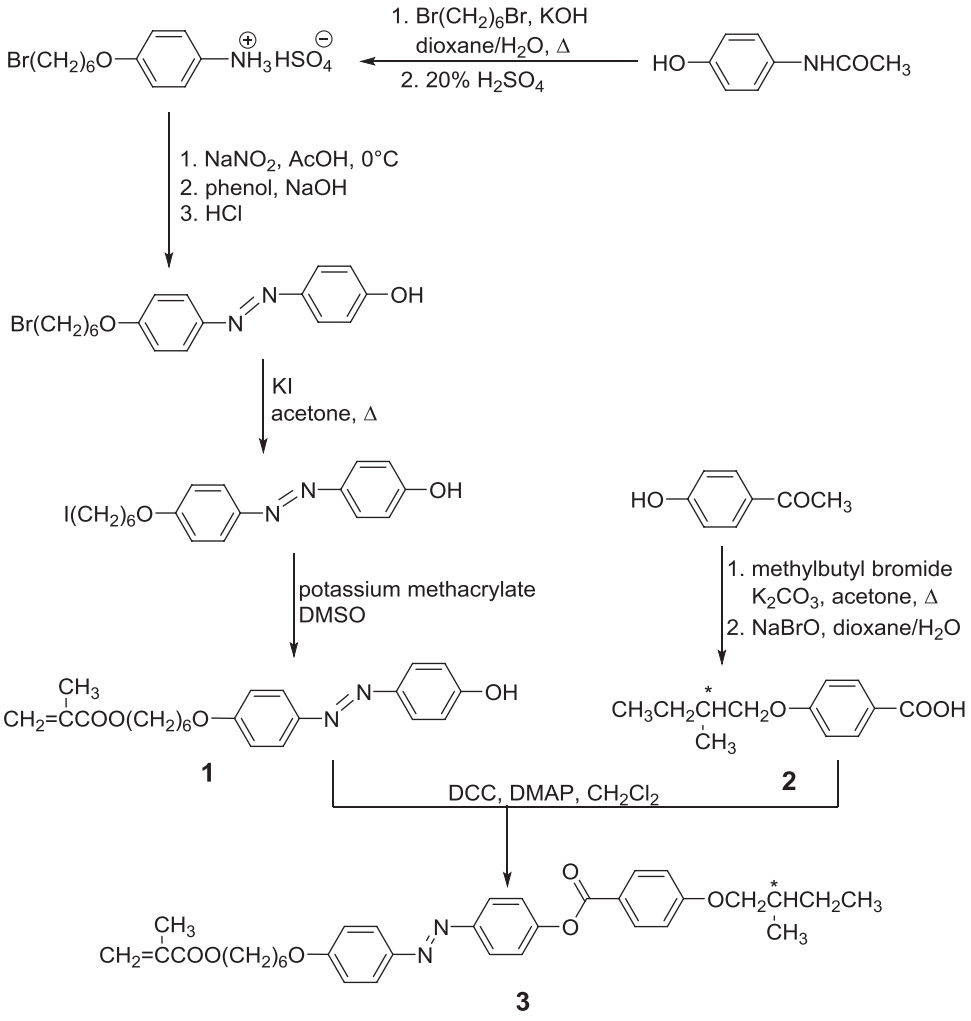

Figure 1. Scheme for synthesis of monomer **MAzo-6**.

MRI TCPU H heating stage), working in a transmission mode, and Bruker GADDS system (CuKα radiation, HiStar area detector) working in a reflection mode. In both systems, the temperature stability was 0.1 K. Powder samples (for Nanostar) were prepared in thin-walled glass capillaries (1.5 mm diameter); partially oriented samples for the experiments in reflection mode were prepared as droplets on a heated surface.

Grazing-incidence wide-angle X-ray scattering (GIWAXS) experiments were performed on polymethacrylate samples at the ID-10 beamline at European Synchrotron Radiation Facility (ESRF) (Grenoble, France). Diffraction patterns were collected with a Pilatus 300k detector (172×172 μm^2 pixel size). The wavelength of 1.24 Å was used. The measurements were performed on thin films deposited on Si substrate at an incidence angle of 0.2° that allows X-ray beam to probe all the thin film volume. The modulus of the scattering s vector ($|s| = 2\sin\theta/l$, where θ is Bragg angle) was calibrated using seven orders of Ag behenate for WAXS and three orders for small angle X-ray scattering (SAXS). In situ heating ramps were performed with a Linkam heating stage. For in situ UV-irradiation, Herolab UV-8S/L lamp (254&365 nm wavelength, 680 and 950 μW cm^{-2}) placed directly above the sample at ≈5 cm distance was used. Integration of 2D WAXS patterns was performed with home-made routines built in Igor Pro software (Wavemetrics Ltd.).

Thin polymer films were deposited on Si substrate by spin-coating using solutions in chloroform at 10 mg mL^{-1} concentration with 1000 rot min^{-1} speed to obtain film thickness of ≈100 nm. In order to completely remove all traces of chloroform, the spin-coated films were kept at room temperature for 1 d. Fibers were drawn from the molten drop at a temperature of 190 °C.

For selective light reflection study, the polymer films were prepared between two glass plates coated with polyvinyl alcohol and rubbed in one direction in order to achieve a good planar alignment. The film thickness was predetermined by the use of 20 μm thick Teflon spacers. Before investigation, the films were annealed during 30 min 10 °C below the clearing point followed by slow cooling down (1° min^{-1}). Transmittance spectra were recorded by Hitachi U3400 UV–vis–atomic force microscopy (near infrared) spectrophotometer.

The surface morphology of polymer films was investigated with FemtoScan scanning probe microscope in semicontact mode of atomic force microscopy (AFM) in air at room temperature.

Cantilevers (MikroMasch) with the average resonant frequency of 325 kHz and tip radius of curvature of about 10 nm were used.

2.4. Photo-Optical Investigations

Thin polymer films for photo-optical experiments were obtained by spin-coating using chloroform solutions of different concentrations. In order to completely dry, the spin-coated films were kept at room temperature for 1 d. The film thickness was estimated from the UV–vis spectral data to be in the range of 100–200 nm.

Photochemical investigations were performed using an optical setup equipped with a DRSh-350 ultrahigh pressure mercury lamp and MBL-N-457 diode laser (457 nm, CNI Laser). To prevent the heating of the samples due to the IR irradiation of the mercury lamp, a water filter was introduced in the optical scheme. To assure the plane-parallel light beam, a quartz lens was applied. Using the filters, a light with the wavelengths 365 and 436 nm was selected. The intensity of light was measured by LaserMate-Q (Coherent) intensity meter and was equal to ≈2.0 mW cm^{-2} (365 nm), ≈1.0 mW cm^{-2} (436 nm) for lamp and ≈0.3 W cm^{-2} for laser.

Spectral measurements were performed using Unicam UV-500 UV–vis spectrophotometer. The linearly polarized spectra of film samples were studied with TIDAS spectrometer (J&M) equipped with rotating polarizer (Glan–Taylor prism controlled by computer program). The dichroism values, D, of the polymer films were calculated from the spectra using the following Equation (1)

$$D = \left(A_{\parallel} - A_{\perp}\right) / \left(A_{\parallel} + A_{\perp}\right) \quad (1)$$

where $A_{\parallel}$ and $A_{\perp}$ are the absorbance parallel and perpendicular to the preferred azobenzene chromophore orientation direction, respectively.

In order to study the out-of plane photo-orientation phenomena, the angular distribution of the polarized absorbance spectra had been measured at an angle of about 45° with respect to the film layer normal.

3. Results and Discussion

3.1. Phase Behavior of the Polymethacrylates

The molecular distribution characteristics of the polymers and their phase behavior are presented in Table 1. According to the polarizing optical microscopy observations and DSC data, both polymethacrylates possess two LC mesophases (cf. Figures S1–S3 in the Supporting Information). At high temperatures, the textures of both polymers reveal the cholesteric phase, which is characterized by focal conics or planar textures with oily streaks and possesses a selective light reflection in the near-IR spectral range (Figure S4, Supporting Information). At lower temperature, values of λ_{max} of both polymers have

Table 1. Phase behavior and molecular masses of the azobenzene-containing polymers. Enthalpies of the phase transitions (in J g^{-1}) measured by DSC on heating (10° min^{-1}) are presented in parentheses.

Material	Phase transitions	M_w	M_w/M_n
PMAzo-6	**SmĈ*** 176 °C (3.3) **N*** 228 °C (1.2) **I**	15 400	1.86
PMAzo-10	**SmX(1)*** 138 °C (5.3) **SmX(2)*** 160 °C (2.1) **N*** 210 °C (1.1) **I**	20 600	1.97

tendency to increase, demonstrating helix untwisting due to the formation of smectic order fluctuations. The low-temperature phase of **PMAzo-6** polymethacrylate has an unspecific texture (Figure S2, Supporting Information), whereas **PMAzo-10** polymethacrylate forms a fan-shaped texture after prolonged annealing (Figure S3, Supporting Information).

GIWAXS was employed to explore the mesophase structure of both polymers. Figure 2 shows 2D GIWAXS diffraction pattern measured on a thin polymer film prepared by spin-coating and subsequently annealed at 150 °C overnight. The diffraction pattern contains information on two different molecular organization levels: a series of peaks in the small-angle region reflects the layer-like organization of the mesogens at a large scale, whereas the broad peak (halo) at wide angles (4.4 Å) corresponds to local organization of the mesogen in the direction perpendicular to the mesogen long axes, similarly to liquid-like order.

For **PMAzo-6** polymethacrylate, a group of diffraction peaks in the small-angle region infers the formation of a particular layer-like structure (Figure 2a). It can be suggested that layers possess a wavy interface, which gives rise to splitting of the 110 and 210 reflexes about the meridional direction of the pattern. Comparing obtained results with the literature data, it is possible to conclude that this phase has a structure similar to the so-called **SmĈ** mesophase.[34] In this rather exotic phase, the mesogens are organized in undulated smectic layers with a liquid-like order within the layers.

The cell parameters of **PMAzo-6** polymethacrylate are as follows: a = 43.3 Å, b = 26.9 Å, γ = 78°. In Table 2, the calculated and experimental d-spacing values are presented. There is a good match between the experimental and calculated values, obtained by fitting experimental peaks and by modeling the X-ray pattern from fitted lattice. Figure 3a schematically represents a possible model for corresponding molecular arrangement and the observable diffraction peaks. It is noteworthy that the mesogen length is close to one half of the corresponding unit cell parameter (i.e., the a-parameter). The number of mesogens per layer was calculated from the macroscopic density measured by flotation method (1.13 g cm^{-3}) and was found to be equal to six.

While comparing the mesogen-length and a-parameter, it is possible to observe the difference which can

Macromol. Chem. Phys. **2017**, DOI: 10.1002/macp.201700127

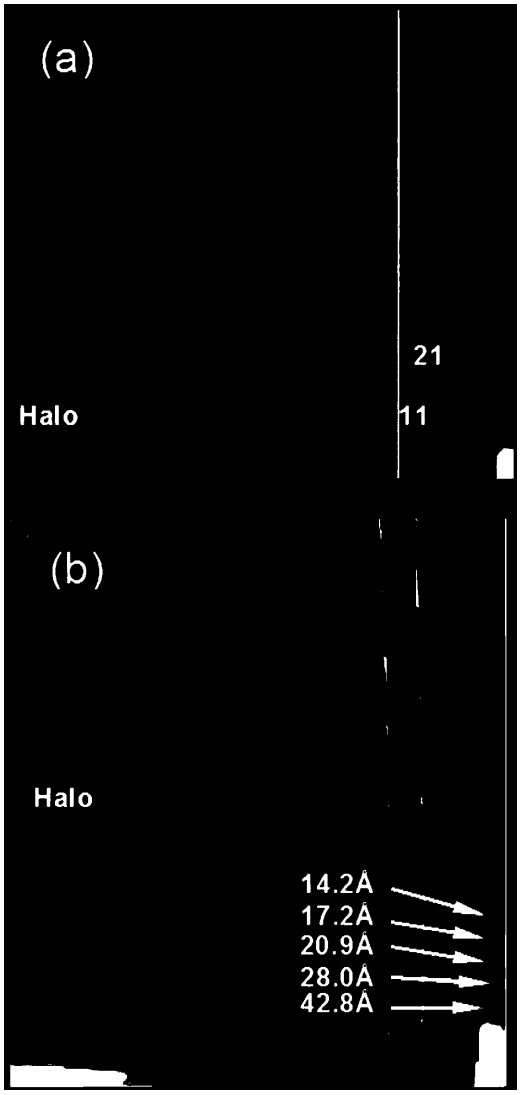

Figure 2. 2D grazing-incidence X-ray patterns corresponding to room-temperature measurements of annealed spin-coated films (the Miller indices are presented) for a) **PMAzo-6** and b) **PMAzo-10** polymethacrylates (different orders of smectic peak are shown).

Table 2. Calculated and experimental *d*-spacing values for 2D unit cell of **PMAzo-6** polymethacrylate.

Miller indices		*d* [Å] (experimental value)	*d* [Å] (calculated value)
H	K		
1	1	24.8	24.8
2	0	21.1	21.1
3	0	14.1	14.1
2	1	18.5	18.5

be related to mesogen tilt inside the layer. Additional experimental evidence for the inclination of the side-chain segments in the structure of **PMAzo-6** polymethacrylate can be obtained from X-ray measurements on uniaxially oriented samples (i.e., fibers). Indeed, a 2D diffractogram given in Figure S5 (Supporting Information) clearly exhibits azimuthal splitting of the halo at 4.4 Å. The tilt of separated parts of scattering from 90° direction indicates the mesogen packing in chevron-like structures, i.e., they form a wave-like layer.

PMAzo-10 polymethacrylate also forms a bilayered structure, which however can be considered as a conventional. This can be confirmed by observation of several orders of the smectic peak (cf. Figure 2b) with the fundamental distance of 85.18 Å. This value was obtained by extrapolation of the diffraction orders because corresponding peak is located out of experimental range of our equipment. The diffraction peak positions are given in Table 3, and the phase structure is schematically shown in Figure 3b.

The temperature-dependent GIWAXS patterns correlate well with the DSC data (cf. Figure S6 in the Supporting Information). The **N*–I** phase transition at high temperatures were not observed on the integrated X-ray patterns due to absence of the halo peak within the measurement range. Two smectic phases observed below the transition to the **N*** phase were designed as the **SmX(1)*** and **SmX(2)*** phases, respectively. The transition between these two smectic phases (at 138 °C) visible on the corresponding DSC trace (Figure S2b, Supporting

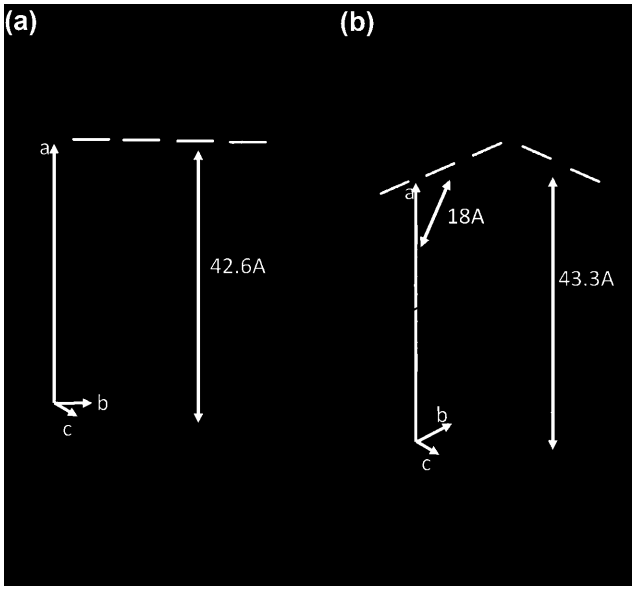

Figure 3. Schematic representation of a possible mesogen packing in the a) **SmĈ*** phase of **PMAzo-6** and b) **SmX(1,2)*** phases of **PMAzo-10** polymethacrylates. Dashed lines show the smectic layer borders.

Macromol. Chem. Phys. **2017**, DOI: 10.1002/macp.201700127

Table 3. Calculated and experimental interlayer distances obtained for smectic **SmX(1)*** and **SmX(2)*** phases for **PMAzo-10** polymethacrylate.

Order number	1	2	3	4	5	6	Diffuse halo [Å]
d, exp., [Å], **SmX(1)***	–	42.78	28.02	20.94	17.19	14.23	4.45
d, calc., [Å], **SmX(1)***	85.18	42.59	28.39	21.29	17.03	14.19	–
d, exp., [Å], **SmX(2)***	–	–	28.02	–	–	14.23	4.45
d, calc., [Å], **SmX(2)***	83.18	41.81	28.02	21.13	16.99	14.23	–

Information), gives rise to a substantial modification of the X-ray diffractogram.

Thus, the first, second, fourth, and fifth orders of the fundamental smectic peak disappear from the patterns (cf. Figure S6b in the Supporting Information). Since the positions of the remaining diffraction peaks did not change, this modification reflects the internal layer reorganization, which may be induced by enhanced mobility of the alkyl chains. Therefore, the observed structural evolution may consist of modification of the relative thickness of the sublayers pertinent to the mesogen and alkyl regions of the system, without changing the total smectic layer thickness.

3.2. Influence of *E–Z* Photoisomerization of the Azobenzene Chromophores in Polymer Films on the Mesophase Behavior

The main absorbance peaks of the polymethacrylate films demonstrate asymmetric shoulders (Figure 4 and Figure S7 (Supporting Information)), that could be explained by the formation of the aggregates.[18,25] UV-irradiation of polymethacrylate films induces *E–Z* isomerization of azobenzene chromophores which is confirmed by significant changes in absorbance spectra presented in Figure 4 and Figure S7 (Supporting Information). Strong decrease in absorbance corresponding to π–π^* electronic transition (337 nm) and increase in peak intensity for

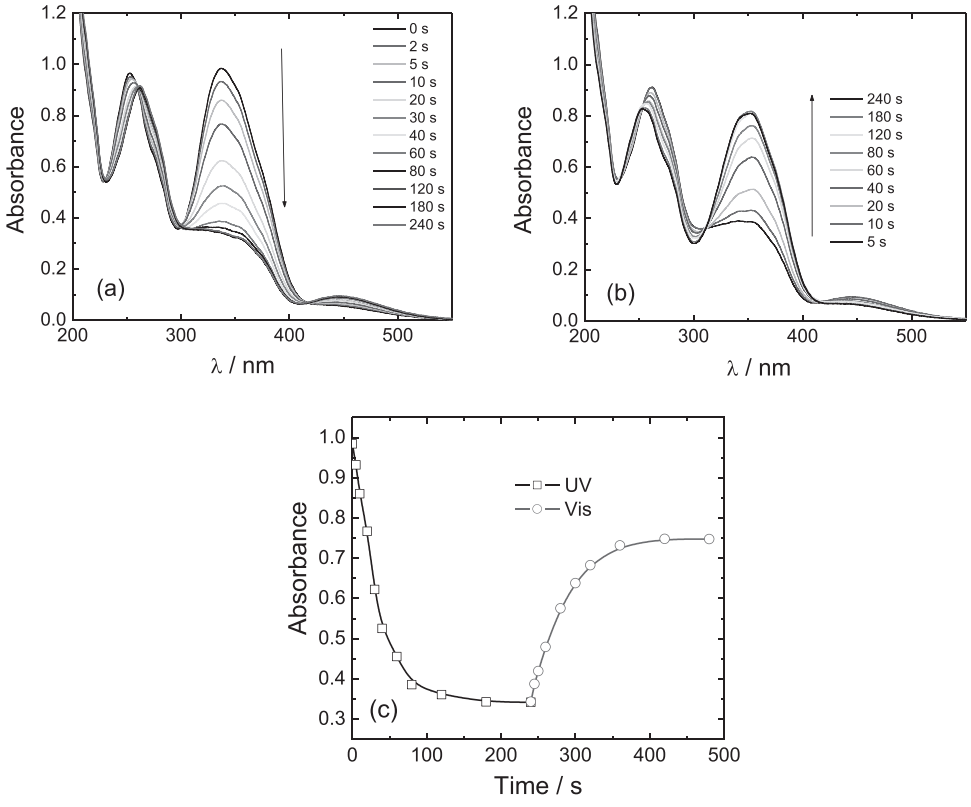

Figure 4. a) Spectral changes under UV-irradiation of amorphousized film of **PMAzo-6** polymethacrylate (365 nm, 4.5 mW cm^{-2}). b) Spectral changes under visible irradiation of UV-irradiated fresh film (436 nm, ≈2.0 mW cm^{-2}). c) Kinetics of absorbance changes.

Macromol. Chem. Phys. **2017**, DOI: 10.1002/macp.201700127

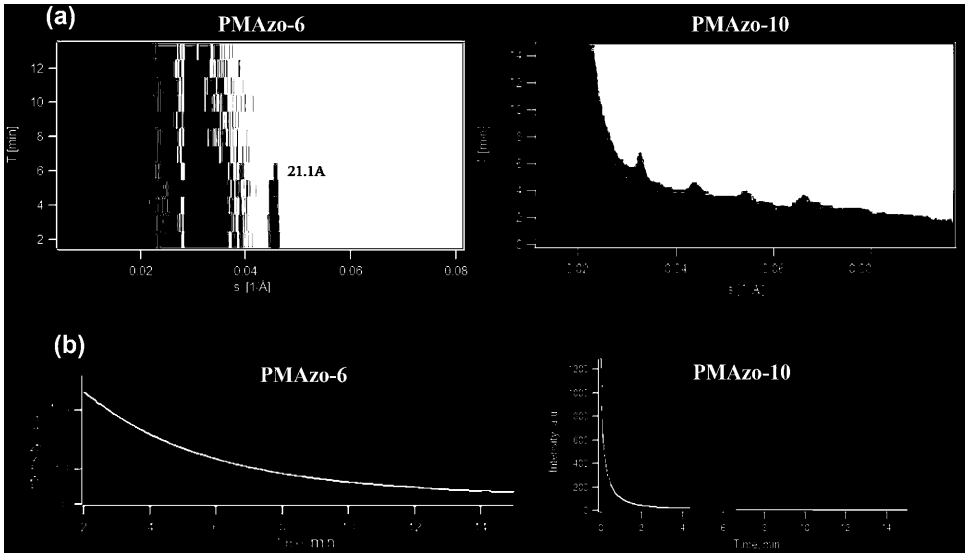

Figure 5. a) Evolution of the integrated intensity of diffraction peaks during UV-irradiation of polymer films; b) intensity decrease for the peak 110 (**PMAzo-6)** and first **Sm** order (**PMAzo-10**) under UV-irradiation (experimental curve is given in black; the red curve stands for the fit to the exponential function).

n–π^* electronic transition (≈450 nm) are clearly observed in the spectra.

According to results obtained by X-ray scattering, the smectic structure of thin annealed films of **PMAzo-6** polymethacrylate gradually disappears during UV-irradiation (Figure 5a). This effect is associated with a decrease in the azobenzene groups' anisometry during *E–Z* isomerization. The *Z*-isomers having low anisometry destroy the LC-order. The decrease of smectic 110 peak intensity for **PMAzo-6** polymethacrylate is well described by the exponential law (Figure 5b, red curve), whereas for **PMAzo-10** polymethacrylate, a substantial deviation from exponential law has been found. The characteristic transition time calculated from fitting process was found to be about 6 min. Annealing of the films induces recovery of the initial LC-state.

Photoinduced phase transition in **PMAzo-6** polymethacrylate enables to control surface topography of polymer films. Figure 6a,b shows AFM scans of the polymer film surface before and after UV-irradiation. Ridge-like structures (with width of 740 ± 110 nm and the height of 60 ± 20 nm) were observed on the film surface before UV-irradiation. In the direction perpendicular to the ridges, periodic height changes with a step length of 90–150 nm have been found. The latter is associated with the smectic order in **PMAzo-6** polymethacrylate as it disappears after UV-irradiation, and is reforming back after annealing. After UV-irradiation, the ridges are broadened; their average height increases to 130 ± 30 nm (Figure 6b). The mean-square roughness of the surface grows from 20 to 60 nm.

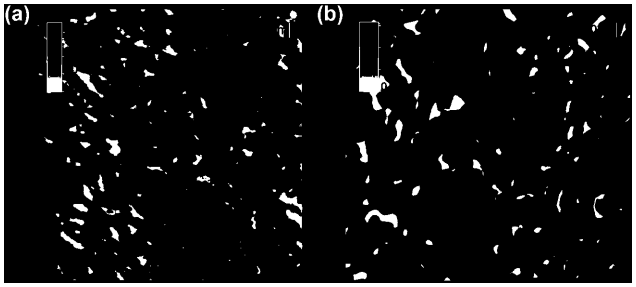

Figure 6. AFM scans of **PMAzo-6** polymethacrylate film a) before and b) after UV-irradiation (365 nm, 4.5 mW cm^{-2}, 30 min).

In contrast, **PMAzo-10** polymethacrylate films have smooth isotropic surface, consisting of polymer blobs with the height of ≈1 nm and the size of ≈30 nm in the surface plane (Figure S8a, Supporting Information). The films contain some bumps and pores (Figure S9b, Supporting Information), which probably get up during the preparation process. No significant changes of the surface morphology of **PMAzo-10** polymethacrylate film were observed after UV-irradiation.

Thus, spacer length plays a very significant role in the topography changes under UV-irradiation of polymer films. Probably, separation of the chromophores from the polymer backbone by the longer flexible spacer in **PMAzo-10** polymethacrylate completely suppresses formation of any features in surface topography as well as their changes during *E–Z* photoisomerization.

3.3. Photo-Orientation and Reorientation Processes in Polymer Films under Polarized Light Action

Irradiation of amorphousized spin-coated polymethacrylate films by polarized blue light (457 nm laser)

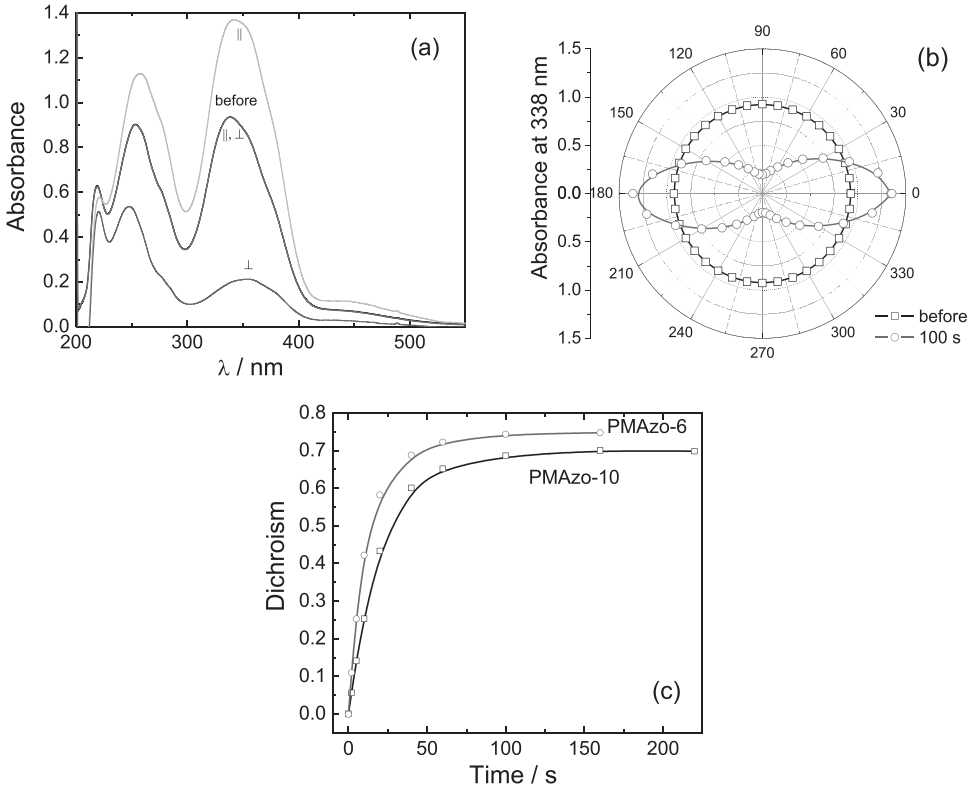

Figure 7. a) Polarized absorbance spectra for **PMAzo-6** polymethacrylate before and after irradiation (100 s). b) Polar plot of polarized absorbance for **PMAzo-6** polymethacrylate. c) Kinetics of dichroism growth for both studied polymethacrylates.

induces photo-orientation process, i.e., alignment of azobenzene chromophores in direction perpendicular to the polarization plane of the incident light. This effect becomes apparent as strong dichroism in absorbance of the polarized light (Figure 7a,b and Figure S9 (Supporting Information)). It is noteworthy that rate of the dichroism growth is a little bit higher for **PMAzo-6** polymethacrylate (Figure 7c). The obtained values of the dichroism are very large and noticeably higher than for the previously studied polyacrylate with the same chromophore (0.75 vs 0.57).[18]

A significant difference was found in thermal stability of the photoinduced dichroism. Thus, annealing of the irradiated samples of **PMAzo-10** polymethacrylate at 120 °C (temperature corresponding to the **SmX(1)*** phase) leads to slight decrease in dichroism values (to 0.57), whereas for **PMAzo-6** polymethacrylate, *D* values increases up to 0.91. This thermal behavior of the irradiated films is completely different in comparison with the previously studied polyacrylate with the identical chromophore structure.[18] For the polyacrylate, an annealing was found to fully disrupt photoinduced alignment due to the transition to homeotropic state (with chromophores oriented along normal to the film plane).

Alternate rotation of polarization plane of excitation light allows one to realize many cycles of chromophore reorientation in both amorphousized and annealed polymer films (Figure 8). At each irradiation cycle, polarization plane is rotated by 90° with respect to the previous one. Important peculiarities, namely the decrease of the orientation rate and maximal achievable dichroism value after first irradiation cycle (≈0.6 instead ≈0.75) can be observed in Figure 8b,c. This phenomenon is associated with partial out-of-plane chromophore orientation which is confirmed by measurements of the polarized absorbance spectra of the film tilted by 45° with respect to the probe beam (Figure S10, Supporting Information). Reorientation occurs through the out-of-plane oriented state (at ≈60 s of irradiation) for both amorphousized and annealed films. Investigation of the reorientation phenomena in amorphous and annealed LC polymer films showed that in annealed films, reorientation proceeds is slower but the maximal values of *D* remain about the same (Figure 9), i.e., LC state of the film slows down the rate of the reorientation, but does not suppress chromophore alignment.

Thus, irradiation of polymer films enables to achieve strong uniaxial alignment of the chromophores with extremely high values of the photoinduced dichroism. Alternate rotation of polarization plane of excitation light during photo-orientation experiments allows making many cycles of chromophore reorientation. Investigations of the kinetics of this process have revealed influence of

Macromol. Chem. Phys. **2017**, DOI: 10.1002/macp.201700127

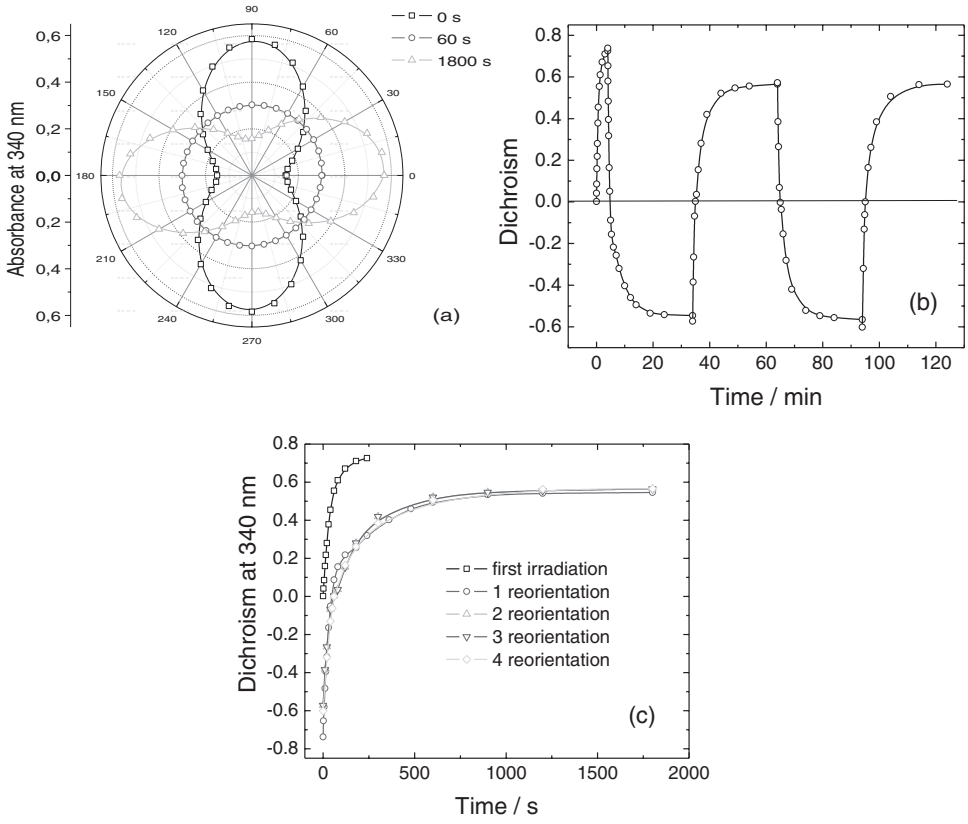

Figure 8. a) Polar plot of polarized absorbance during reorientation process in amorphousized **PMAzo-6** polymethacrylate film (457 nm, ≈50 mW). b,c) Dichroism changes during first irradiation and after subsequent reorientation cycles. Subfigure (c) shows the difference in the rate of the first irradiation and subsequent reorientation cycles.

LC-order of the films on the rate of this process, however the values of the photoinduced dichroism are the same for amorphous and LC-films.

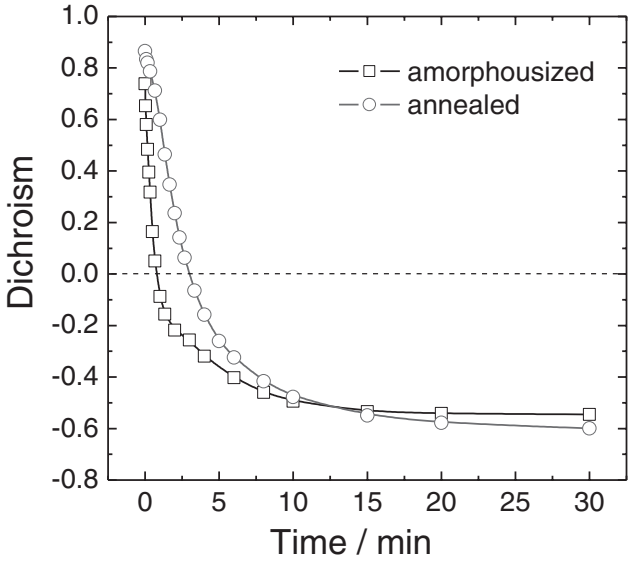

Figure 9. Comparison of reorientation process kinetics for amorphousized and annealed **PMAzo-6** polymethacrylate films.

4. Conclusions

Two new azobenzene containing chiral monomers and corresponding LC polymethacrylates with azobenzene-containing side groups with different spacer length, 6 and 10 methylene groups (**PMAzo-6** and **PMAzo-10**, respectively) were obtained. Their mesomorphic behavior and photo-optical properties were studied. POM, DSC, and X-ray investigations reveal formation of different smectic phases and a broad temperature range of the cholesteric phase.

UV-irradiation induces effective reversible *E–Z* photo-isomerization in polymer solutions and films. As was shown by AFM study, UV-irradiation of polymer films results in noticeable changes in the surface topography of **PMAzo-6** polymethacrylate film, whereas for **PMAzo-10** polymethacrylate film, surface remains unchanged. Irradiation by polarized blue light (457 nm) results in photo-orientation process in polymer films resulting in significant alignment of the chromophores in direction perpendicular to the polarization plane of the incident light. The significant difference was found in thermal stability of the photoinduced alignment; an annealing of the irradiated samples of **PMAzo-10** polymethacrylate leads to slight decrease in dichroism values (to 0.57), whereas

for **PMAzo-6**, polymethacrylate dichroism increases up to very high values (0.91).

For the first time, the reorientation process in azobenzene-containing polymers induced by polarized light with alternate changing of the direction of the polarization plane was studied. A possibility of performing cycles of reorientation without any fatigue has been demonstrated. Further studies related to this topic are in progress now and will be presented elsewhere.

Supporting Information

Supporting Information is available from the Wiley Online Library or from the author.

Acknowledgements: This research was supported by the Russian Foundation for Basic Research (grant nos. 16-03-00455, 16-29-05140, study of photo-optical properties of PAAzo) by the Russian Science Foundation (14-13-00379, study of the phase behavior of the polymers) and Scholarships of the President of the Russian Federation for young scientists and graduate students (№SP-2238.2016.1, study of the mesophases structure by X-ray). Authors (V.H. and A.B.) greatly acknowledge the financial support from the MEYS LH15305 and the CSF 16-12150S research projects.

Conflict of Interest: The authors declare no conflict of interest.

Received: March 11, 2017; Revised: April 17, 2017; Published online: ; DOI: 10.1002/macp.201700127

Keywords: azobenzene; liquid crystalline polymers; photoisomerization; photo-orientation phenomena

[1] H. K. Bisoyi, Q. Li, *Chem. Rev.* **2016**, *116*, 15089.
[2] T. Seki, *J. Mater. Chem. C* **2016**, *4*, 7895.
[3] V. P. Shibaev, *Polym. Sci., Ser. A* **2014**, *56*, 727.
[4] H. M. D. Bandarab, S. C. Burdette, *Chem. Soc. Rev.* **2012**, *41*, 1809.
[5] A. Sobolewska, S. Bartkiewicz, J. Mysliwiec, K. D. Singer, *J. Mater. Chem. C* **2014**, *2*, 1409.
[6] J. Jaworska, S. Bartkiewicz, Z. Galewski, *J. Phys. Chem. C* **2013**, *117*, 27067.
[7] D.-Y. Kim, D.-G. Kang, M.-H. Lee, J.-S. Kim, C.-R. Lee, K.-U. Jeong, *Chem. Commun.* **2016**, *52*, 12821.
[8] F. Fernandez-Palacio, M. Poutanen, M. Saccone, A. Siiskonen, G. Terraneo, G. Resnati, O. Ikkala, P. Metrangolo, A. Priimagi, *Chem. Mater.* **2016**, *28*, 8314.
[9] E. Uchida, K. Sakaki, Y. Nakamura, R. Azumi, Y. Hirai, H. Akiyama, M. Yoshida, Y. Norikane, *Chem. - Eur. J.* **2013**, *19*, 17391.
[10] M. Czajkowski, K. Dradrach, S. Bartkiewicz, Z. Galewski, *Opt. Mater.* **2013**, *35*, 2449.
[11] J. Guan, M. Zhang, B. Li, H. Yang, G. Wang, *ChemPhysChem* **2012**, *13*, 3812.
[12] D.-Y. Kim, S.-A. Lee, H. Kim, S. M. Kim, N. Kim, K.-U. Jeong, *Chem. Commun.* **2015**, *51*, 11080.
[13] A. Kozanecka-Szmigiel, J. Konieczkowska, D. Szmigiel, K. Switkowski, M. Siwy, P. Kuszewski, E. Schab-Balcerzak, *Dyes Pigm.* **2015**, *114*, 151.
[14] E. Bagherzadeh-Khajeh Marjan, S. Ahmadi-Kandjani, M.S. Zakerhamidi, J.-M. Nunzi, *Opt. Mater.* **2014**, *38*, 228.
[15] J. Royes, C. Provenzano, P. Pagliusi, R. M. Tejedor, M. Piñol, L. Oriol, *Macromol. Rapid Commun.* **2014**, *35*, 1890.
[16] S. Grebenkin, B. Bol'shakov, V. M. Syutkin, *J. Phys. Chem. B* **2014**, *118*, 9800.
[17] A. Bobrovsky, V. Shibaev, *Liq. Cryst.* **2012**, *39*, 339.
[18] A. Bobrovsky, V. Shibaev, A. Bubnov, V. Hamplová, M. Kašpar, M. Glogarová, *Macromolecules* **2013**, *46*, 4276.
[19] A.V. Bogdanov, A. K. Vorobiev, *J. Phys. Chem. B* **2013**, *117*, 12328.
[20] A. Bobrovsky, N. Boiko, V. Shibaev, *Polymer* **2015**, *56*, 263.
[21] A. Bobrovsky, O. Sinitsyna, S. Abramchuk, I. Yaminsky, V. Shibaev, *Phys. Rev. E* **2013**, *87*, 012503.
[22] O. Sinitsyna, A. Bobrovsky, I. Yaminsky, V. Shibaev, *Colloid Polym. Sci.* **2014**, *292*, 1567.
[23] A. Bobrovsky, K. Mochalov, A. Chistyakov, V. Oleinikov, V. Shibaev, *Macromol. Chem. Phys.* **2012**, *213*, 2639.
[24] A. Bobrovsky, K. Mochalov, A. Chistyakov, V. Oleinikov, V. Shibaev, *J. Photochem. Photobiol., A* **2014**, *275*, 30.
[25] A. Bobrovsky, V. Shibaev, A. Bubnov, D. Pociecha, V. Hamplová, M. Kašpar, M. Glogarová, *Macromol. Chem. Phys.* **2011**, *212*, 342.
[26] T. Toth-Katona, M. Cigl, K. Fodor-Csorba, V. Hamplová, I. Jánossy, M. Kašpar, T. Vojtylová, A. Bubnov, *Macromol. Chem. Phys.* **2014**, *215*, 742.
[27] M. Cigl, A. Bubnov, M. Kašpar, F. Hampl, V. Hamplová, O. Pacherová, J. Svoboda, *J. Mater. Chem. C* **2016**, *4*, 5326.
[28] A. Bobrovsky, V. Shibaev, M. Cigl, V. Hamplová, D. Pociecha, A. Bubnov, *J. Polym. Sci., Part A: Polym. Chem.* **2016**, *54*, 2962.
[29] S. Menghetti, M. Alderighi, G. Galli, F. Tantussi, M. Morandini, F. Fusob, M. Allegrini, *J. Mater. Chem.* **2012**, *22*, 14510.
[30] R. J. Knarr III, G. Manfredi, E. Martinelli, M. Pannocchia, D. Repetto, C. Mennucci, I. Solano, M. Canepa, F. B. de Mongeot, G. Galli, D. Comoretto, *Polymer* **2016**, *84*, 383.
[31] L. B. Braun, T. G. Linder, T. Hessberger, R. Zentel, *Polymers* **2016**, *8*, 435.
[32] S. Palagi, A. G. Mark, S. Y. Reigh, K. Melde, T. Qiu, H. Zeng, C. Parmeggiani, D. Martella, A. Sanchez-Castillo, N. Kapernaum, F. Giesselmann, D. S. Wiersma, E. Lauga, P. Fischer, *Nat. Mater.* **2016**, *15*, 647.
[33] C. L. van Oosten, C. W. M. Bastiaansen, D. J. Broer, *Nat. Mater.* **2009**, *8*, 677.
[34] N. Boiko, V. Shibaev, B. Ostrovskii, S. Sulyanov, D. Wolff, J. Springer, *Macromol. Chem. Phys.* **2001**, *202*, 297.